

REDUCTION OF ELECTROMAGNETIC FIELD RADIATED BY POWER ELECTRONIC CONVERTERS

M. Melit^{1,*}, B. Nekhou¹, N. Boudjerda¹,
K. E. Khamlichi Drissi², and K. Kerroum²

¹Department of Electrical Engineering, LAMEL Laboratory, University of Jijel, Jijel, Algeria

²LASMEA Laboratory, Blaise Pascal University, Aubière, France

Abstract—This paper is concerned with a modeling technique of electromagnetic radiations of power electronics circuits during a switching operation of a power electronic component. The electromagnetic radiating loops are formed by PCB traces assumed to be perfect conductor. We complete our study by proposing a technique using passive loops to reduce the magnetic field emitted by the power electronic converter. To achieve this, we propose to solve Maxwell's equations by using the FDTD method where open boundaries, dielectric board and ground plane are taken into consideration. A validation of the model used in our work (solving Maxwell equations using FDTD) is realized by comparison with other theoretical concepts.

1. INTRODUCTION

During the completion operation of a switch in electrical circuits, the emitted electromagnetic fields cause a transient voltage induced on the target circuit and may be amplified thus producing an annoying disturbance; particularly the fast variation of current is responsible for an inductive coupling.

To protect electrical circuits from this disturbance phenomenon of magnetic induction:

- Firstly, we aim to minimize areas of all loops, both the emitting loops and target loops;

Received 24 April 2011, Accepted 30 June 2011, Scheduled 24 July 2011

* Corresponding author: Mohammed Melit (melit@univ-jijel.dz).

- We sometimes try to oppose a magnetic field H by submitting a “short-circuited loop”. However, its influence is relative since it leads to an attenuation and does not eliminate the problem;
- Finally and most importantly, we can significantly reduce the inductive coupling by enclosing the sensitive part or disruptive in a metal casing.

For devices of power electronics, the second solution “short-circuited loop” seems interesting because it can be realized directly on the PCB, and it is not expensive, but may be inefficient if its dimensions are not optimal.

In this work, we propose the modeling of electromagnetic radiation emitted by the current loops which appear in the circuits of power electronics during the operation of a switch and the effect of a short circuited loop.

This problem is well known and discussed in the literature. Classically, numerical modeling in the frequency domain is used with the marketed codes of simulation (NEC, FEKO ...); this modeling consists of getting a solution of the integral equation by the moment method [1] where the Fast Fourier Transform (FFT) is useful in the frequency domain.

In a recent work [2], we were interested to calculate the electromagnetic field by an analytic method. To simplify the modeling and take into account the nonlinearities associated with the switch operation, we propose, in this work, to address the problem directly in the time domain using the concept of discretization of Maxwell's equations proposed by Yee [3]. This technique is widely used for the computation of electromagnetic field in various domains [4, 5].

The device that we study is generally composed of traces forming loops, an insulating support and a conductor ground plane. We solve Maxwell's equations by FDTD in each element of the device while taking into account the open boundaries using absorbent conditions [6].

The introduction of a “short circuited loop” in the device does not complicate the modeling because it is treated as a simple conductor in the same way as the traces.

The presence of the “short-circuited loop” requires only to modify the physical characteristics of the line in the three-dimensional mesh. This advantage allows us to vary the dimensions of the additional loop to optimize the reduction effect of the magnetic field.

To illustrate our work, first we present some validations, then we propose some applications of the electromagnetic radiation, and finally we introduce passive loops to analyze the reduction of this problem.

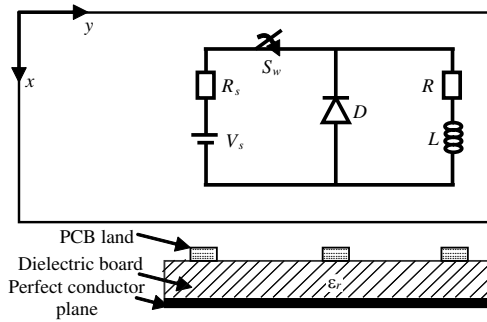


Figure 1. Typical geometry of the power converter.

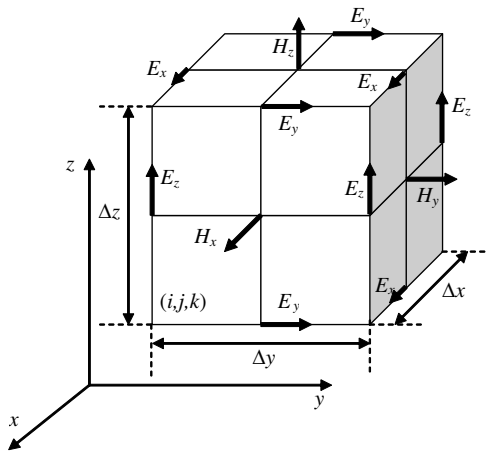


Figure 2. K. S. Yee Cell.

2. SOLUTION OF MAXWELL EQUATIONS BY FDTD

The geometry of a typical power converter circuit (buck converter) is illustrated in Fig. 1, where V_s is the voltage source; R_s is the source resistor; S_w denotes the switch component; and R and L represent the resistor and the inductor of the load respectively, while D represents a free-wheel diode.

Considering the geometry of power electronic converter (Fig. 1), the computation of electromagnetic field radiated by this circuit is not a fast process due to the fact that it contains nonlinear lumped elements (Diode, transistor), dielectric layer and PCB traces. In the time domain, numerical computation can be obtained based on the solution of Maxwell equations by the Finite Difference Time Domain

(FDTD) method. The Maxwell curl equations can be written as:

$$\text{rot}\vec{E} = -\mu\frac{\partial\vec{H}}{\partial t} \quad (1)$$

$$\text{rot}\vec{H} = \sigma\vec{E} + \varepsilon\frac{\partial\vec{E}}{\partial t} \quad (2)$$

Yee [3] introduces a set of finite difference equations for the system of scalar equations equivalent to Maxwell's equations in the Cartesian coordinate system. To perform all of the space derivatives, Yee evaluates E and H at alternate half-time steps (Fig. 2).

Due to the finite capabilities of the computers used to implement the FDTD method, the mesh must be limited in three directions x , y , and z . The Maxwell curl equations discretized using the central-difference method cannot be used to evaluate the tangential components of the electric field at the outer boundaries since they require the values of the magnetic field components outside of the mesh [6].

2.1. Absorbing Boundary Conditions

In the configurations treated in this paper, one of the six mesh boundaries of the computation domain is a perfect ground plane, and its tangential electric field values are forced to be zero [7]. The tangential electric field components on the other five mesh walls must be specified in such a way that the outgoing waves are not reflected; this problem can be solved by using the absorbing boundary conditions as described in [6].

In our work, we have opted for using the first order Mur's absorbing boundary condition [6]. Therefore, the finite difference approximation of z -component of the electric field for plane $x = 0$ is expressed by Equation (3) as follows:

$$\begin{aligned} & E_z^{n+1}\left(0, j, k + \frac{1}{2}\right) \\ &= E_z^n\left(1, j, k + \frac{1}{2}\right) + \frac{c\Delta t - \Delta x}{c\Delta t + \Delta x} \left[E_z^{n+1}\left(1, j, k + \frac{1}{2}\right) - E_z^n\left(0, j, k + \frac{1}{2}\right) \right] \quad (3) \end{aligned}$$

2.2. Handling Components for Applying FDTD Method

FDTD method is extensively used for calculating electromagnetic problems since Yee first proposed it in 1966 [3]. We have applied the FDTD method in 3-D for calculating the electromagnetic fields distribution. In this case, some problems must be solved to (i) deal

with the printed circuit traces; (ii) handle the dielectric boards; (iii) handle some kinds of lumped loads including linear loads, such as resistor, capacitor and inductor, and nonlinear loads, such as diode and electronic switch. This approach is described in literature [8].

2.2.1. Dealing with the Dielectric Board

In 1988, Taflove et al. [9] first proposed a method, called contour integral approach which is derived from Maxwell’s integral equations (Fig. 3).

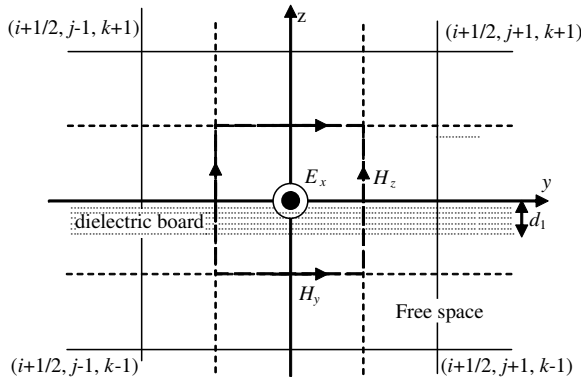


Figure 3. Using contour integral approach to model dielectric board.

This approach allows to derive the FDTD equation in an inhomogeneous medium which includes both the free space and the dielectric board.

$$\begin{aligned}
 & E_x^{n+1} \left(i + \frac{1}{2}, j, k \right) \\
 = & \frac{T_{ax2}}{T_{ax1}} E_x^n \left(i + \frac{1}{2}, j, k \right) \\
 & + \frac{1}{T_{ax1} \Delta y} \left[H_z^{n+\frac{1}{2}} \left(i + \frac{1}{2}, j + \frac{1}{2}, k \right) - H_z^{n+\frac{1}{2}} \left(i + \frac{1}{2}, j - \frac{1}{2}, k \right) \right] \\
 & - \frac{1}{T_{ax1} \Delta z} \left[H_y^{n+\frac{1}{2}} \left(i + \frac{1}{2}, j, k + \frac{1}{2} \right) - H_y^{n+\frac{1}{2}} \left(i + \frac{1}{2}, j, k - \frac{1}{2} \right) \right] \quad (4)
 \end{aligned}$$

with:

$$\begin{aligned}
 T_{ax1} &= \frac{\varepsilon_0}{\Delta t} \left(1 - \frac{d_1}{2\Delta z} \right) + \frac{d_1 \cdot \varepsilon_1}{2\Delta t \cdot \Delta z} + \frac{d_1 \cdot \sigma_1}{4\Delta z} \\
 \text{and } T_{ax2} &= \frac{\varepsilon_0}{\Delta t} \left(1 - \frac{d_1}{2\Delta z} \right) + \frac{d_1 \cdot \varepsilon_1}{2\Delta t \cdot \Delta z} - \frac{d_1 \cdot \sigma_1}{4\Delta z} \quad (5)
 \end{aligned}$$

Equation (4) means that to update the tangential electric field component at the interface, we need to estimate only the average of the relative permittivities and conductivities on each side cell.

Other electric field components can also be obtained by the same method.

2.2.2. The Printed Circuit Traces

This section considers the problem of an E -polarized plane wave incident on a thin resistive strip of width w along x -axis and of resistance R as shown in Fig. 4.

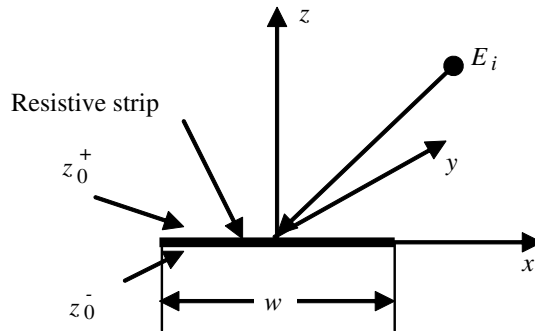


Figure 4. An E -polarized plane wave illumination of a thin resistive strip of width w and resistance R .

The boundary conditions can be written as:

$$E_y(x, y, z_{0+}) = E_y(x, y, z_{0-}) = E_y(x, y, z_0) = -RJ_y(x, y, z_0) \quad (6)$$

$$J_y(x, y, z_0) = H_x(x, y, z_{0+}) - H_x(x, y, z_{0-}) \quad (7)$$

J_y : the total (y -directed) electric current density on the surface of the strip.

In our case, the PCB trace has a very high conductivity, so these electric conductors can be assumed perfectly conducting and with zero thickness. As such, this case can simply be treated by setting the electric field components that lie on the conductors to zero [7]. Through extensive numerical experimental testing, it is demonstrated that this method is suited to our applications.

2.2.3. Linear Lumped Components

The power converter circuit considered in this paper includes linear lumped elements (resistor, voltage source with internal resistors).

Using the FDTD method, the lumped elements may be accounted in Maxwell’s equations by starting with Ampere’s equation [8].

For a resistive load, we consider it to be oriented in the x -direction. Therefore, the finite difference approximation for x -component of the electric field can be expressed by Equation (8):

$$\begin{aligned}
 & E_x^{n+1} \left(i + \frac{1}{2}, j, k \right) \\
 &= \frac{\left(\frac{\varepsilon_0}{\Delta t} - \frac{\Delta x}{2R\Delta y\Delta z} \right)}{\left(\frac{\varepsilon_0}{\Delta t} + \frac{\Delta x}{2R\Delta y\Delta z} \right)} E_x^n \left(i + \frac{1}{2}, j, k \right) \\
 &+ \frac{1}{\left(\frac{\varepsilon_0}{\Delta t} + \frac{\Delta x}{2R\Delta y\Delta z} \right)} \frac{\left[H_z^{n+1/2} \left(i + \frac{1}{2}, j + \frac{1}{2}, k \right) - H_z^{n+1/2} \left(i + \frac{1}{2}, j - \frac{1}{2}, k \right) \right]}{\Delta y} \\
 &- \frac{1}{\left(\frac{\varepsilon_0}{\Delta t} + \frac{\Delta x}{2R\Delta y\Delta z} \right)} \frac{\left[H_y^{n+1/2} \left(i + \frac{1}{2}, j, k + \frac{1}{2} \right) - H_y^{n+1/2} \left(i + \frac{1}{2}, j, k - \frac{1}{2} \right) \right]}{\Delta z} \quad (8)
 \end{aligned}$$

For a voltage source with an internal resistor, we consider that it is also oriented in the x -direction. Therefore, the finite difference approximation for x -component of the electric field is expressed by Equation (9):

$$\begin{aligned}
 & E_x^{n+1} \left(i + \frac{1}{2}, j, k \right) = \frac{\left(\frac{\varepsilon_0}{\Delta t} - \frac{\Delta x}{2R_s\Delta y\Delta z} \right)}{\left(\frac{\varepsilon_0}{\Delta t} + \frac{\Delta x}{2R_s\Delta y\Delta z} \right)} E_x^n \left(i + \frac{1}{2}, j, k \right) + \frac{\frac{\Delta t}{R_s\varepsilon_0\Delta y\Delta z}}{1 + \frac{\Delta t\Delta x}{2R_s\varepsilon_0\Delta y\Delta z}} \\
 &+ \frac{1}{\left(\frac{\varepsilon_0}{\Delta t} + \frac{\Delta x}{2R_s\Delta y\Delta z} \right)} \frac{\left[H_z^{n+1/2} \left(i + \frac{1}{2}, j + \frac{1}{2}, k \right) - H_z^{n+1/2} \left(i + \frac{1}{2}, j - \frac{1}{2}, k \right) \right]}{\Delta y} \\
 &- \frac{1}{\left(\frac{\varepsilon_0}{\Delta t} + \frac{\Delta x}{2R_s\Delta y\Delta z} \right)} \frac{\left[H_y^{n+1/2} \left(i + \frac{1}{2}, j, k + \frac{1}{2} \right) - H_y^{n+1/2} \left(i + \frac{1}{2}, j, k - \frac{1}{2} \right) \right]}{\Delta z} \quad (9)
 \end{aligned}$$

3. NUMERICAL SIMULATIONS

3.1. Validation

At the first stage, we propose a validation of our numerical results (obtained by solving Maxwell equations using FDTD) by comparing with other theoretical concept published in [10].

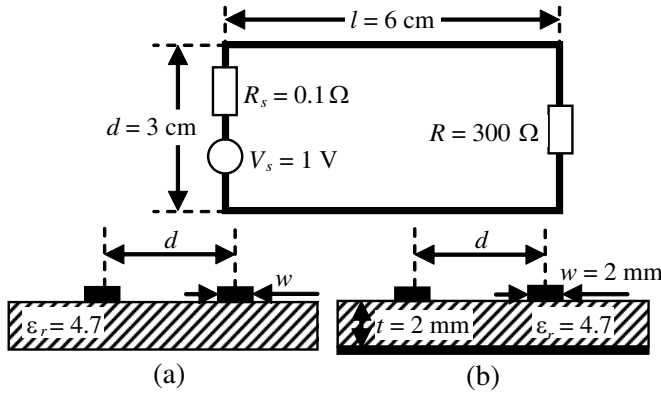


Figure 5. Configuration of the circuits used for simulation. (a) Without ground plane. (b) With ground plane

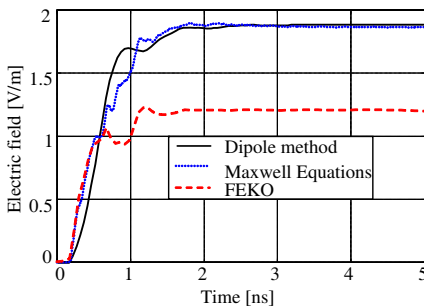


Figure 6. Electric field radiated by the circuit without ground plane.

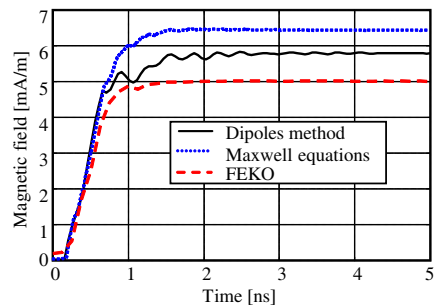


Figure 7. Magnetic field radiated by the circuit without ground plane.

The analyzed circuit is illustrated in Fig. 5 for both cases: with and without ground plane. First, we consider an ideal switch, and the turn-on process is modeled by taking a step signal (V_s) with a rise time $t_r = 0.5$ ns.

3.1.1. Circuit Without Ground Plane

In Fig. 6 and Fig. 7, we present the results of electric and magnetic fields variations in the center of the circuit and at 5 cm above the circuit board.

The two approaches directly implemented in the time domain

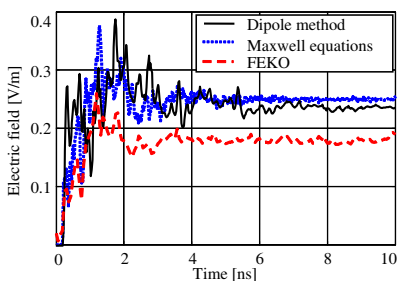


Figure 8. Electric field radiated by the circuit with ground plane.

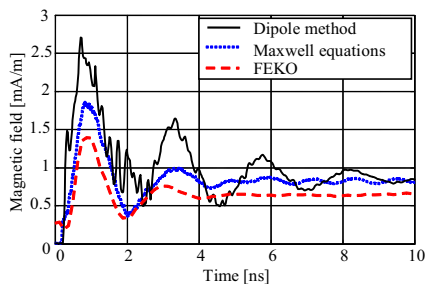


Figure 9. Magnetic field radiated by the circuit with ground plane.

(Hertzian dipoles and the solution of Maxwell’s equations by FDTD) give very close results in both the shape and amplitude (Fig. 6 and Fig. 7). The slight difference between the two calculations is certainly made by the spatial and temporal discretizations when using the FDTD and the superposition principle to the concept of dipoles [10].

Using FEKO software [11] and Fourier transform for modeling in the time domain, one can observe that the general shape is conserved, but the magnitude is decreased at the end of rise time (established regime). This result is predictable because the use of the FFT for the transition frequency-time and vice versa requires to take into account very special precautions (sampling frequency, sufficient number of points, continued decreasing . . .), which otherwise can seriously affect the results.

3.1.2. Circuit with Ground Plane

For this simulation, we consider the geometric configuration in Fig. 5(b) with ground plane and the same point for calculating the electromagnetic field.

In Fig. 8 and Fig. 9, we give the results of electric and magnetic fields.

The introduction of the ground plan highlights the significant difference among the three formalisms. The difference between the calculations directly in the time domain and those obtained using the software FEKO can be justified by using the Fourier transform. For the magnetic field, one can see a slight difference between the two temporal methods; this difference shows that the method of multiple images adapts well especially for the calculation of the electric field in the event that we have a perfectly ground plane.

3.2. Application

3.2.1. Effect of Geometric Configuration of the Circuit

To see the effect of the geometric configuration of the power converter circuit on the radiated electromagnetic field, we propose its application directly as an example. Let's consider the three geometric configurations in Fig. 10, which represent the same circuit under different shapes. It is worth noting that we have kept the same perimeter for all configurations.

We calculate the electric and magnetic fields emitted by each configuration in Fig. 10 by solving Maxwell's equations using the FDTD method at the center of the loop and 5 cm in height (Fig. 11 and Fig. 12).

The analysis of these results (Fig. 11 and Fig. 12) shows that the geometric placement of the traces considerably affects the converter's

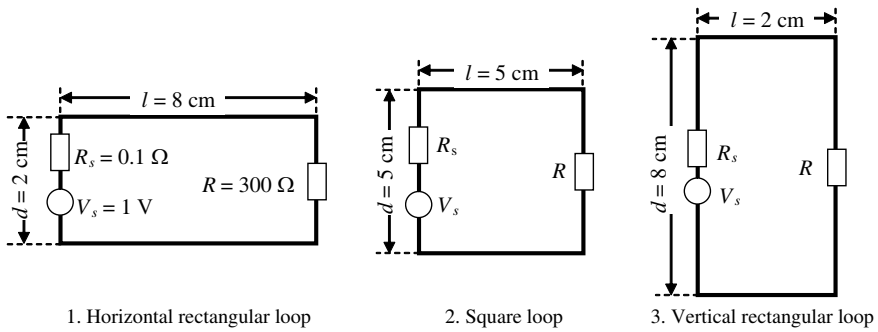


Figure 10. Geometric configurations of the converter's circuit.

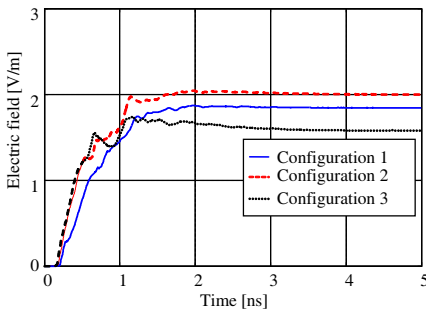


Figure 11. Electric field for the three configurations.

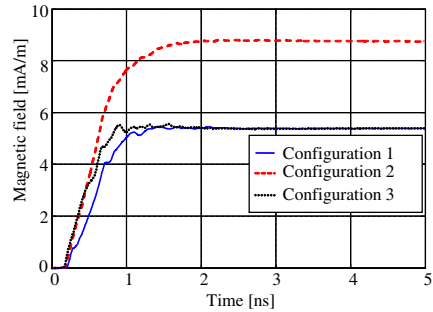


Figure 12. Magnetic field for the three configurations.

radiation. Indeed, the spectral content caused by different transients when changing the geometry of the radiating loop can lead to a significant difference in both electric and magnetic fields obtained by different geometric configurations. This effect is significant in the magnetic field; the largest loop (configuration 2) results in the largest magnetic emission (note that the magnetic moment is proportional to the surface of the loop). For the electric field, the distribution of the surface charges on the traces is in our view directly related to their positions vis-à-vis the source and their respective lengths (in this case, the coefficients depend only on potential geometry).

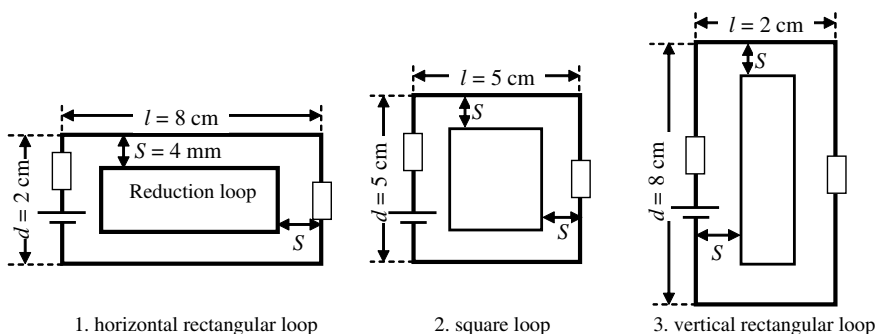


Figure 13. Different geometric configurations of the converter circuit with passive loop.

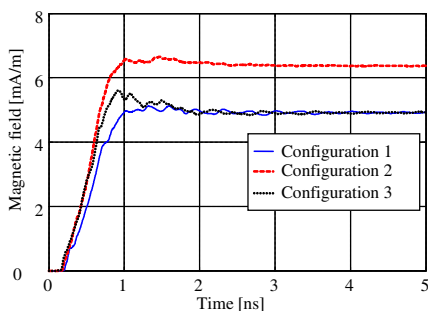


Figure 14. Reduced magnetic field for the three geometric configurations.

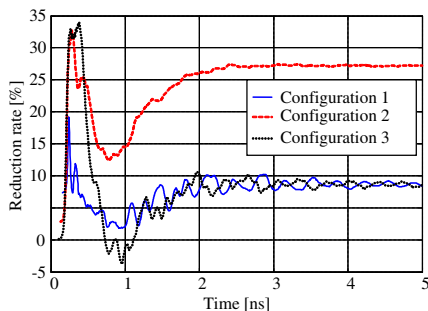


Figure 15. Reduction rate of the magnetic field for the three geometric configurations.

3.2.2. Effect of One Passive Loop

We propose in this application the reduction of the magnetic field by a simple passive loop introduced inside the converter for the three geometric configurations illustrated in Fig. 13.

In Fig. 14, we give the calculated magnetic fields, and in Fig. 15, we present the reduction rate produced by the passive loop for the three configurations.

It can be noted that the effect of the reduction is much greater in the square loop (configuration 2). From this result, we have already

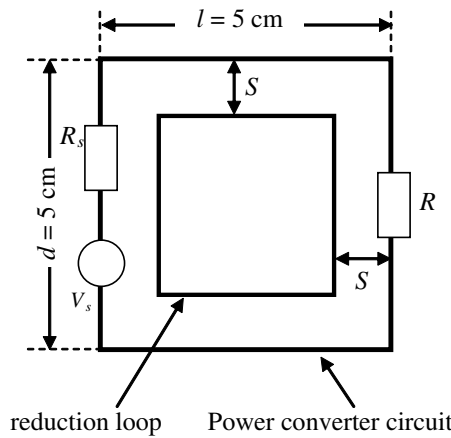


Figure 16. Configuration of the power converter circuit with passive loop.

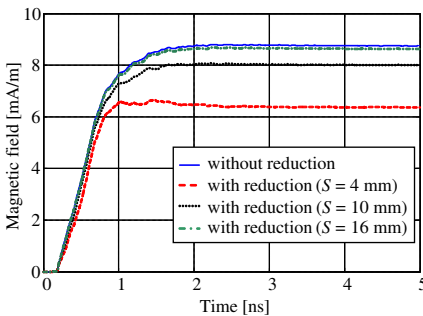


Figure 17. Reduced magnetic field according to the passive loop size.

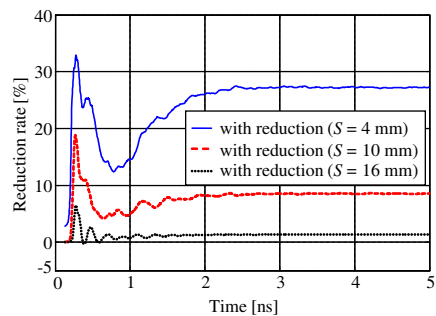


Figure 18. Reduction rate of the magnetic field according to the passive loop size.

said that in terms of EMC, for the same perimeter, a rectangular circuit with passive loop reduction is a first solution.

3.2.3. Effect of the Loop Size on the Passive Reducing

In this application, we investigate the effect of the size (area) of the passive reduction loop (Fig. 16) where the reduction loop is short circuited. We have perform our calculations for values of $S = 4\text{ mm}$, 10 mm and 16 mm , respectively (Fig. 16) for the case of configuring the worst in terms electromagnetic radiation (square circuit).

Figures 17 and 18 clearly show that the passive loop which leads to the largest reduction is the one with the most important radiating surface.

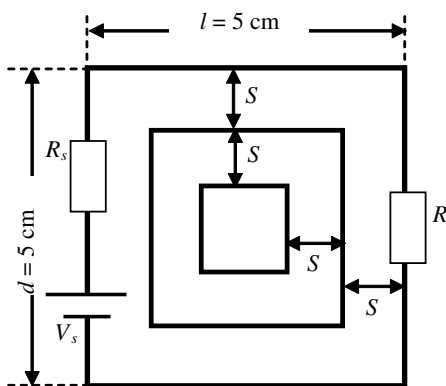


Figure 19. Configuration of a power circuit with two reduction loops.

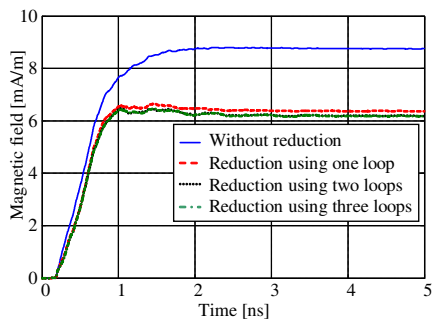


Figure 20. Reduced magnetic field (effect of the number of passive loops).

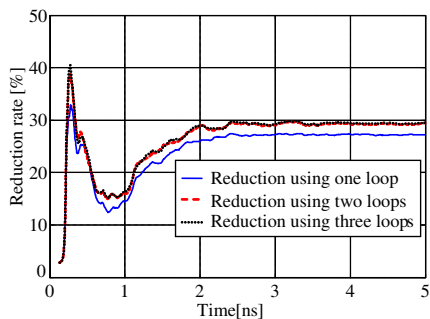


Figure 21. Reduction rate of the magnetic field.

3.2.4. *Effect of the Number of Passive Loops on the Reduction*

We propose in this application to analyze the effect of the overlapping of multiple loops on the reduction, as shown in Fig. 19.

The results illustrated in Figs. 20 and 21 show that increasing the number of passive loops does not continually and significantly reduce the magnetic field.

3.2.5. *Effect of Resistive Loads at the Ends of the Reduction Loop*

For this application, considering the most unfavorable configuration in terms of electromagnetic radiation (square loop), we investigate the

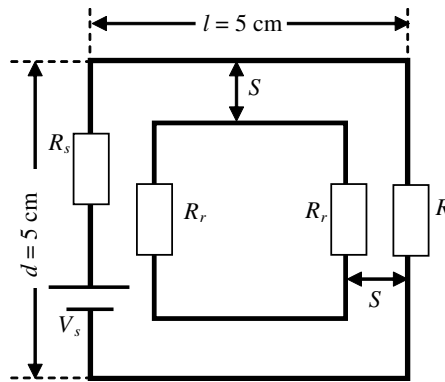


Figure 22. Electric circuit of the power converter with reduction loop loaded with resistors at both ends.

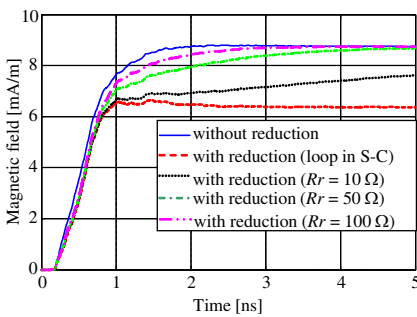


Figure 23. Reduced magnetic field for different values of load at the ends of the passive loop.

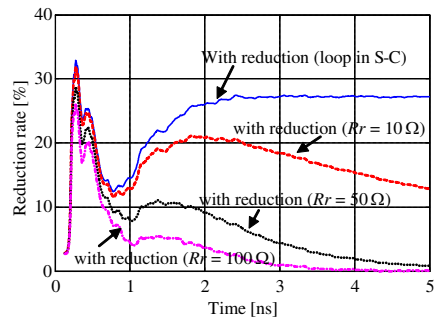


Figure 24. Reduction rate of the magnetic field for different values of loads at the ends of the passive loop.

effect of loads at both ends of the passive loop (Fig. 22).

From these results (Figs. 23 and 24), we can say that a simple loop short-circuited at both ends is the first EMC solution. For the same passive loop, the configuration where both ends are short-circuited leads to induced currents of larger amplitudes

4. CONCLUSION

This paper proposes novel methods for the reduction of electromagnetic perturbations radiated by power electric converters. The first technique is based on the geometric configuration of the electric circuit of the converter while the second method consists in the placement of passive loops directly in the converter circuit.

The modeling of the problem is based on the solution of Maxwell equations by FDTD and requires the meshing of the volume with different materials (air, dielectric, conductor ...). The choice of the space increment in 3D is imposed by the stability criterion [12] required when using the FDTD method. Considering the fast switches used in the power electronics circuits, the choice of an appropriate step time imposes a fine spatial discretization, which inevitably leads to high computation time and sometimes to numerical noises.

As a result, we can conclude that the geometric placement of traces can be the first solution for the EMC, and the adding of passive loops reduces the electromagnetic emission of the power converter considerably.

REFERENCES

1. Degauque, P. and J. Hamelin, "Compatibilité électromagnétique, bruit et perturbations radioélectriques," BORDAS et C.N.E.T.-E.N.S.T, ISBN 2-04-018807-X, Dunod, Paris, 1990.
2. Melit, M., B. Nekhoul, N. Boudjerda, K. E. K. Drissi, and K. Kerroum, "Investigation of electromagnetic emission in power converters," *International Review of Electrical Engineering (I.R.E.E.)*, Vol. 2, No. 2, 203–216, April 2007.
3. Yee, K. S., "Numerical solution of initial boundary value problems involving Maxwell's equations in isotropic media," *IEEE Trans. Antennas Propag.*, Vol. 14, 302–307, May 1966.
4. Zhang, Y.-Q. and D.-B. Ge, "A unified FDTD approach for electromagnetic analysis of dispersive objects," *Progress In Electromagnetics Research*, Vol. 96, 155–172, 2009.

5. Yang, S., Y. Chen, and Z.-P. Nie, "Simulation of time modulated linear antenna arrays using the FDTD method," *Progress In Electromagnetics Research*, Vol. 98, 175–190, 2009.
6. Mur, G., "Absorbing boundary condition for the finite-difference approximation of time-domain electromagnetic field equations," *IEEE Trans. Electromag. Compact.*, Vol. 23, 377–382, November 1981.
7. Sheen, D. M., S. M. Ali, M. D. Abouzahra, and J. A. Kong, "Application of the three-dimensional finite-difference time-domain method to the analysis of planar microstrip circuits sheen," *IEEE Trans. Microwave Theory Tech.*, Vol. 38, No. 7, 849–857, July 1990.
8. Picket-May, M., A. Taflove, and J. Baron, "FD-TD modelling of digital signal propagation in 3D circuits with passive and active loads," *IEEE Trans. Microwave Theory Tech.*, Vol. 42, No. 8, 1514–1523, Aug. 1994.
9. Taflove, A., K. R. Umshankar, and K. S. Yee, "Detailed FD-TD analysis of electromagnetic fields penetrating narrow slots and lapped joints in thick conducting screens," *IEEE Trans. Antennas Propag.*, Vol. 36, No. 2, 247–257, Feb. 1988.
10. Melit, M., B. Nekhoul, N. Boudjerda, K. Kerroum, and K. E. K. Drissi, "Computation of electromagnetic field radiated by power electronic converters," *EMC Europe 2008*, 23–28, Hambourg, Germany, 2008.
11. FEKO, EM Software & Systems GmbH, Otto-Lilienthal-Strasse 36, D-71034 Böblingen, Allemagne.
12. Taflove, A. and M. E. Brodwin, "Numerical solution of steady-state electromagnetic scattering problems time-difference time dependent Maxwell's equations," *IEEE Trans. Microwave Theory Tech.*, Vol. 23, 623–630, Aug. 1975.